



Influence of thermal treatment on tensile failure of basalt fibers

Jiří Militký *, Vladimír Kovačič, Jitka Rubnerová

Faculty of Textile Sciences, Technical University of Liberec, Halkova 6, Liberec CZ 461 17, Czech Republic

Abstract

In this contribution selected ultimate tensile properties of basalt fibers are presented. Properties are investigated after tempering to the 50, 100, 200, 300 °C. Scanning electron microscopy identifies structural changes of fibers. The distribution of stress at break is described by the Weibull type model. It was postulated that fracture occurs due to nonhomogeneities in fiber volume (probably near the small crystallites of minerals). The analysis of fibrous fragment evolved during abrasion of basalt weave is presented. Despite of fact that basalt particle are too thick to be respirable the handling of basalt fibers must be carried out with care. © 2002 Elsevier Science Ltd. All rights reserved.

Keywords: Basalt fibers; Thermo mechanical analysis; Strength distribution; Fiber failure; Particle size analysis

1. Introduction

Basalt fibers, similarly to glass fibers, can be used for production of high temperature resistant and chemically inactive products. The main problems of basalt fibers preparation are the gradual crystallization of some structural parts (plagioclase, magnetite, pyroxene) and the nonhomogeneity of melt [6,7]. Basalt is therefore still used mainly for molded products (flag stones, pipes) with increased abrasion resistance, temperature resistance and chemical resistance. Basalt is used also in a form of short fibers for insulation purposes (basalt wool). Basalt filament yarns are therefore used only rarely.

The technology of continuous spinning can overcome the problems with unevenness and resultant filament yarns can be used in the textile branch. It is possible to use these yarns for production of planar or 3D textile structures for composites, special knitted fabrics and also as the sewing threads. Especially an application of basalt yarns as the sewing threads is very attractive. It is possible to use these threads for joining of filtering bags for hot media, filtering bags for very aggressive chemical environment, etc. Fresh basalt fibers are practically amorphous. Due to action of high temperature these fibers have ability to partially crystallize. This modified form of basalt fibers can be more brittle and the strength can be too low [3,4,12].

In this contribution selected properties of basalt fibers in the comparison with glass ones are presented. Ultimate tensile mechanical properties were investigated at room temperature and after tempering to the 50, 100, 200, 300, 400 and 500 °C. The strength distribution of basalt filaments was described by the three

* Corresponding author. Fax: +48-535-3542.

E-mail address: jiri.militky@vslib.cz (J. Militký).

parameter Weibull type model of fibers. Tensile failure mode is identified with scanning electron microscopy. The analysis of fibrous fragment evolved during abrasion of basalt weave is presented.

2. Basalt fibers

Basalt is generic name for solidified lava poured out of the volcanoes [1,2,5]. Basaltoid rocks are melted approximately in the range 1500–1700 °C. When this melt is quickly quenched, it solidified to glass like, nearly amorphous, solid. Slow cooling leads to more or less complete crystallization, to an assembly of minerals. Two essential minerals plagiocene and pyroxene make up perhaps 80% of many types of basalt. Classification of basaltoid rocks based on the contents of main basic minerals is described in the book [5]. From the point of view of chemical composition of basalts the silicon oxide SiO₂ (optimal range 43.3–47 wt.%) dominates and Al₂O₃ (optimal range 11–13%) is next in abundance. Content of CaO (optimal range 10–12%) and MgO (optimal range 8–11%) are closely similar. Other oxides are almost always below 5% level.

Basalts are more stable in strong alkalis than glasses. Stability in strong acids is slightly lower. Basalt products can be used from very low temperatures (about –200 °C) up to the comparative high temperatures 700–800 °C. At higher temperatures the structural changes occur.

Basalt rocks from VESTANY hill was used as a raw material in this work. Based on the DTA measurements the crystallization temperatures T_c of individual minerals were evaluated. For magnetite $T_c = 720$ °C, for pyroxene $T_c = 830$ °C and for plagioclase $T_c = 1010$ °C.

A roving with 280 single filaments was prepared. Mean fineness of roving was 45 tex. The basic physical properties of basalt fibers are presented in Table 1.

3. Statistical analysis of fibers strength

The fracture of fibers can be generally described by the micromechanical models or on the base of pure probabilistic ideas [8]. The probabilistic approach is based on these assumptions:

- (i) fiber breaks at specific place due to a critical defect size (catastrophic flaw),
- (ii) defects are distributed randomly along the length of fiber (model of Poisson marked process),
- (iii) fracture probabilities at various places along the length are mutually independent.

The cumulative probability of *fracture* $F(V, \sigma)$ depends on the tensile stress level and fiber volume V . The simple derivation of the stress at break distribution described for example by Kittl and Diaz [9] leads to the general form

$$F(V, \sigma) = 1 - \exp(-R(\sigma)) \quad (1)$$

where $R(\sigma)$ is known as the *specific risk* function. For the well known Weibull distribution this function has the form [14]

Table 1
Basic physical properties of glass and basalt fibers

Property	E-glass	Basalt
Diameter (μm)	9–13	8.63
Density (kg m ⁻³)	2540	2733
Softening temperature (°C)	840	960

$$R(\sigma) = [(\sigma - A)/B]^C \tag{2}$$

where A is the lower strength limit, B is a scale parameter and C is a shape parameter (model WEI 3). For brittle materials is often assumed $A = 0$ (model WEI 2).

Weibull models are physically to be no correct due to unsatisfactory upper limit of strength. Kies [15] proposed more realistic risk function (model KIES) in the form

$$R(\sigma) = [(\sigma - A)/(A1 - \sigma)]^C \tag{3}$$

where $A1$ is upper strength limit. For brittle materials can be also assumed $A = 0$ (model KIES2). Further generalization of $R(p)$ have been published by Phani (model PHA5)

$$R(\sigma) = [(\sigma - A)/B1]D/[(A1 - \sigma)/B]C \tag{4}$$

It can be proved that the B and $B1$ cannot be independently estimated. Therefore the constraint $B1 = 1$ is used in sequel. Simplified version of Eq. (4) has $A = 0$ (model PHA4). For well known Gumbell distribution (GUMB) is $R(\sigma)$ described as

$$R(\sigma) = \exp[(\sigma - A)/(B)] \tag{5}$$

Main aim of the statistical analysis is specification of $R(\sigma)$ and parameter estimation based on the experimental strengths $(\sigma_i) i = 1, \dots, N$.

The individual basalt fibers removed from roving were tested. The loads at break were measured under standard conditions and sample length 10 mm. Load data were transformed to the stresses at break σ_i (GPa). The sample of 50 stresses at break values was used for evaluation of the $R(\)$ functions and estimate of their parameters.

Owing to their special structure the parameters of Weibull type distributions can be estimated by using of the maximum likelihood method. This method is very interesting because of its good statistical properties (asymptotic efficiency, consistency and asymptotic normality of estimators) [10].

For the case when $\sigma_i, i = 1, \dots, N$ are independent random variables with the same probability density function $f(\sigma) = F'(\sigma_i, \mathbf{a})$ the logarithm of likelihood function L (corresponding to simultaneous probability density of all measurements) has the form

$$\ln L = \sum \ln f(\sigma_i, \mathbf{a}) \tag{6}$$

where \mathbf{a} are parameters of corresponding risk function. The MLE estimators \mathbf{a}^* can be obtained by the maximization of $\ln L(\mathbf{a})$. This task can be simply converted to the solving of the set of nonlinear equations (see Ref. [10]). Based on the preliminary computation it has been determined that for basalt fibers strength the Weibull distribution is suitable estimates of \mathbf{a}^* obtained by this way for three and two parameter Weibull distribution are given in Table 2.

The differences between three and two parameter Weibull distribution are identified by the values of maximum likelihood function $\ln L(\mathbf{a}^*)$. The three-parameter Weibull distribution was selected as suitable for glass and tempered samples as well.

Table 2
Parameters of Weibull models calculated by MLE

Model	A (GPa)	B (GPa)	C	$\ln L(\mathbf{a}^*)$
WEI3	0.0641	0.230	1.370	33.50
WEI2	–	0.301	1.829	29.164

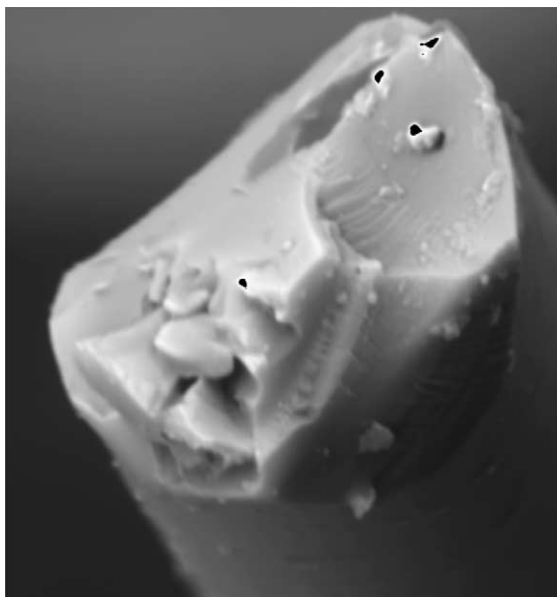


Fig. 1. Fracture plane of glass fiber (magnification: 10000 \times).

4. Fiber failure

Fracture modes of glass and basalt fibers fracture were identified by scanning electron microscopy. The fracture plane of untreated glass fiber is shown in Fig. 1 and fracture plane of untreated basalt fiber is shown in Fig. 2.

The SEM of longitudinal portion of broken fiber (magnification: 10000 \times) is shown in Fig. 3 for basalt and in Fig. 4 for glass. The surface is very smooth without flaws. The SEM of broken fibers after subjecting of temperature 250 °C for 60 min is in Figs. 5 and 6. There are visible nonhomogeneities in the cross-section. Based on these findings we can postulate that fracture occurs due to nonhomogeneities in fiber volume (probably near the small crystallites of minerals).

5. The properties of basalt fibers after the thermal exposure

Maintaining the fibers at the temperature 50, 100, 200, 300 °C for 60 min, simulated behavior of basalt and glass fibers after long-term thermal exposure. After this treatment the following properties was measured:

- tensile strength (N tex⁻¹),
- deformation to break (%),
- dynamic acoustic modulus (Pa) (dynamic acoustic modulus was determined from sound wave spread velocity in the material).

The changes of properties of glass and basalt fibers after tempering were investigated by the analysis of variance. It was determined, that only 300 °C treatment led to statistically significant drop of strength and

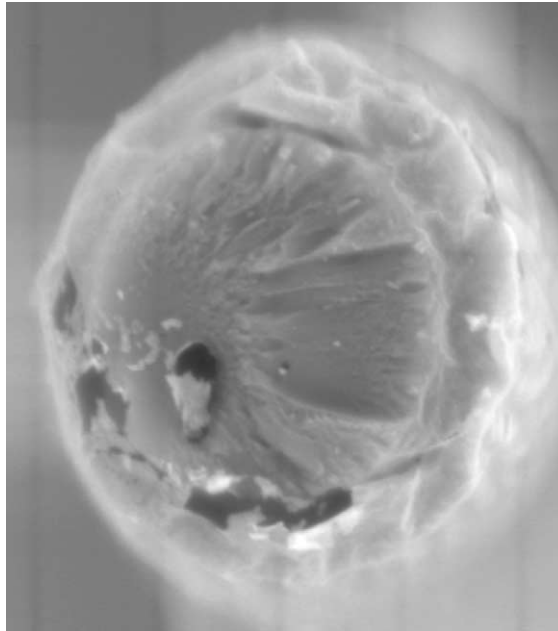


Fig. 2. Fracture plane of basalt fiber (magnification: 10000×).

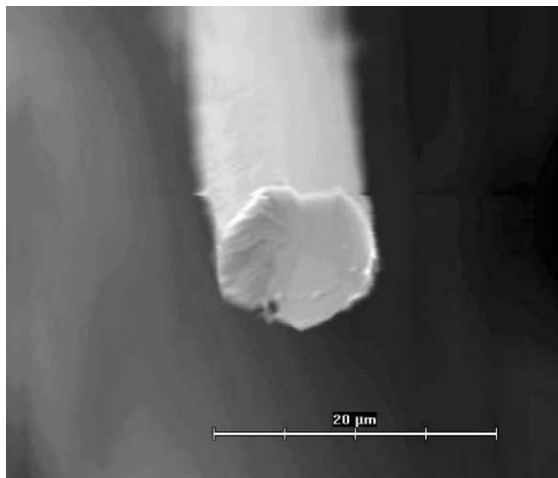


Fig. 3. Longitudinal portion of broken basalt fibers (untreated).

dynamic acoustical modulus. Probably, the changes of these properties are based on the changes in the crystalline structure of fibers.

In the second set of experiments the strength distribution of basalt filament yarns was measured on the samples subjected to temperatures $T_T = 20, 50, 100, 200, 300, 400$ and 500 °C at selected time intervals $t_T = 1, 15,$ and 60 min.

For strength evaluation the TIRATEST 2300 machine was used. Sample of 50 strengths P_i was created. These values were recalculated to stress at break values σ_i (GPa).

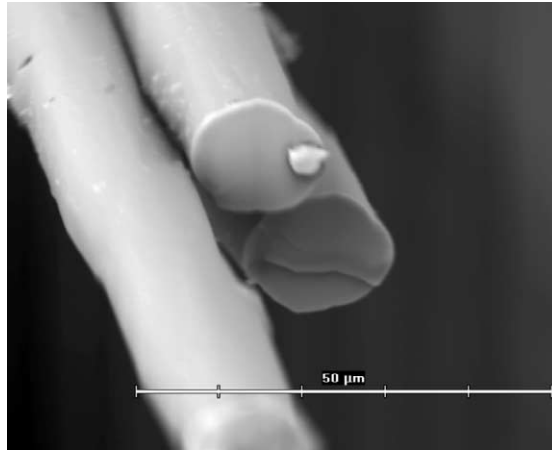


Fig. 4. Longitudinal portion of broken glass fibers (untreated).

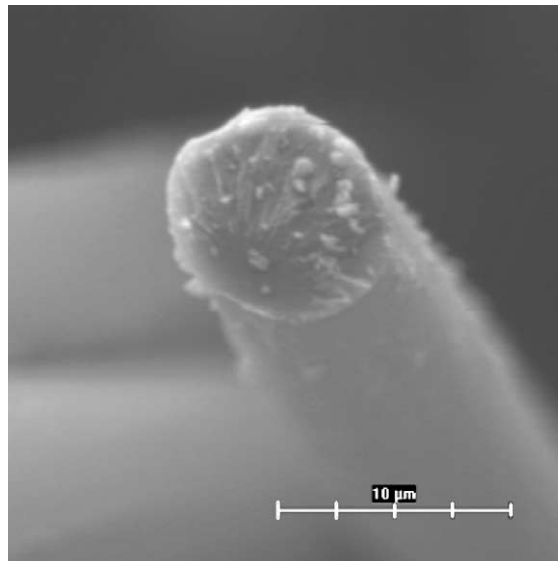


Fig. 5. Longitudinal portion of broken basalt fibers (250 °C for 60 min).

The strength distribution of tempered filament yarns was nearly Gaussian with parameters: mean value σ_p and variance σ^2 . These parameters are estimated by the sample arithmetic mean and sample variance. Results are given in Table 3.

The dependence of the filament yarns strength on the temperature has two nearly linear regions. One at low temperature to the 180 °C with nearly constant strength and one up to the 340 °C with very fast strength drop.

For description of this dependence the linear spline model was used [11]. By the linear least squares the strength σ_1 for temperature $T_1 = 180$ °C and σ_2 for temperature $T_2 = 340$ °C were computed. These values and the rate of strength drop

$$D = (\sigma_1 - \sigma_2)/160 \text{ (GPa deg}^{-1}\text{)} \quad (7)$$

are given in Table 4.

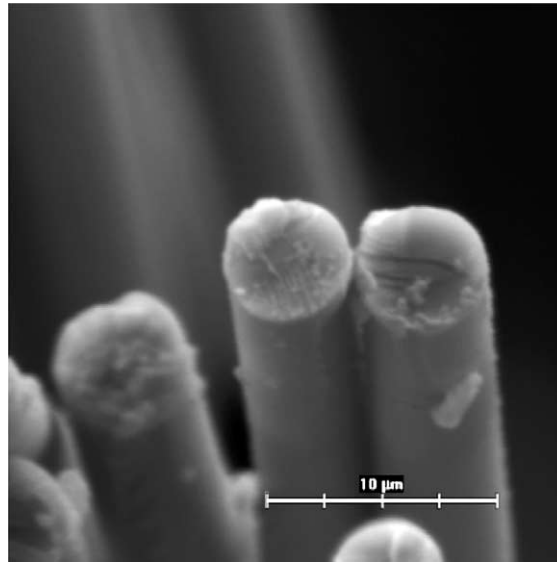


Fig. 6. Longitudinal portion of broken glass fibers (250 °C for 60 min).

Table 3
Parameters of tempered filament yarn strength

T_T (°C)	t_T (min)		15		60	
	1					
	σ_p (GPa)	σ^2 (GPa ²)	σ_p (GPa)	σ^2 (GPa ²)	σ_p (GPa)	σ^2 (GPa ²)
20	1.01	0.0075	1.01	0.0075	1.01	0.0075
50	0.997	0.0110	1.05	0.0110	1.07	0.0150
100	1.03	0.0095	0.991	0.0140	1.01	0.0100
200	0.986	0.0091	1.01	0.0083	1.09	0.0110
300	0.893	0.0140	0.743	0.0150	0.424	0.0100
400	0.743	0.0061	0.701	0.0091	0.112	0.00150
500	0.254	0.0048	0.348	0.0026	0.094	0.00300

Table 4
Thermal dependence of filament yarns strength

t_T (min)	σ_1 (GPa)	σ_2 (GPa)	D (GPa deg ⁻¹)
1	1.0074	0.756	0.0016
15	1.1070	0.343	0.0048
30	1.1750	0.158	0.0064

It is clear that increasing of the time of tempering leads to the acceleration of structural changes and drops of strength fastening (increasing D).

6. Analysis of emitted particles during basalt handling

Some characteristics of the basalt fibers are similar to those of the asbestos. Since the mechanisms for asbestos carcinogenicity are not fully known it cannot be excluded that basalt fibers may also be hazardous

to health. Thus there is a need for analysis of fibrous fragment characteristics in production and handling in order to control their emission.

The fibrous fragments with diameter of $1.5 \mu\text{m}$ or less and length of $8 \mu\text{m}$ or greater should be handled and disposed of using the widely accepted procedures for asbestos. Fibers falling within the following three criteria are of concern [13].

- (a) *The fibers are respirable:* Diameters of $<1.5 \mu\text{m}$ (some say $<3.5 \mu\text{m}$) allow fibers to remain airborne and respirable.
- (b) *The fibers have a length/diameter ratio $R > 3$:* Short stubby fibers (particles) do not seem to cause the serious problems associated with asbestos.
- (c) *The fibers are durable in the lungs:* If fibers are decomposed in the lungs, they do not cause a problem.

Most of nonpolymeric fibers have diameter significantly $>3.5 \mu\text{m}$ but break into long thin pieces. Emission of particles, including fibers, occurs during handling. For simulation of these phenomena the abrasion of basalt weaves were made.

The weave from basalt filaments was used. The fragmentation was realized by the abrasion on the propeller type abrader. Time of abrasion was 60 s. It was proved by microscopic analysis that basalt fibers are not split and the fragments have the cylindrical shape. Fiber fragments were analyzed by the image analysis, system LUCIA M. Only the fragments shorter than $1000 \mu\text{m}$ were analyzed. Results were lengths L_i of fiber fragments. For comparison the diameters D_i of fiber fragments were measured as well.

Basic statistical characteristics fiber fragments lengths are

Mean value $L_M = 230.51 \mu\text{m}$,
 Standard deviation $\sigma_L = 142.46 \mu\text{m}$,
 Skewness $g_1 = 0.969$,
 Kurtosis $g_2 = 3.97$.

These parameters show that the distribution of fiber fragments is unimodal and positively skewed. The same results are valid for distribution of fiber fragments diameters. Basic statistical characteristics of fiber fragments diameters are

Mean value $D_M = 11.08 \mu\text{m}$,
 Standard deviation $\sigma_D = 2.12 \mu\text{m}$,
 Skewness $g_1 = 0.641$,
 Kurtosis $g_2 = 2.92$.

Because the mean value of fiber fragment diameter is the same as diameter of fibers no splitting of fibers during fracture occurs. It is known, that from point of view of cancer hazard the aspect ratio (length/diameter ratio $R = l/d$) is very important. For basalt fiber fragments the aspect ratio $R = 230.51/11.08 = 20.8$. Despite of fact that basalt particle are too thick to be respirable the handling of basalt fibers must be carried out with care.

7. Conclusion

In this contribution the selected properties of basalt fibers in the comparison with glass ones were presented. The properties were investigated after subjecting of fibers to the 50, 100, 200 and 300 °C. The ultimate strength, deformation to break and sound wave spread velocity were measured. The health

problems with this class of fibers are not known. Very long thin fragments of basalt can be dangerous when will be inhaled.

Acknowledgements

This work was supported by the Czech National Grant Agency (grant no. 106/97/0372) and research project of Czech Ministry of Education J11/98:244101113.

References

- [1] Douglas RW, Ellis B. Amorphous material. London: Wiley; 1972.
- [2] Kopecký L, Voldán J. Crystallization of melted rocks. Prague: CSAV; 1959.
- [3] Rubnerová J. Thermomechanical properties of inorganic fibers. Diploma work, TU Liberec; 1996.
- [4] Militký J et al. Proceedings of the International Conference on Special Fibers, Lodz; 1997.
- [5] Morse SA. Basalts and phase diagrams. New York: Springer; 1980.
- [6] Krutsky N et al. Geol Pruzkum 1980;22:33 [in Czech].
- [7] Slivka M, Vavro M. Ceramics 1996;40:149 [in Czech].
- [8] Wagner HD. Stochastic concept in the study of the effect in the mechanical strength of the highly oriented polymeric materials. J Polym Sci Phys B 1989;27:115.
- [9] Kittl P, Díaz G. Weibull fracture statistics or probabilistic strength of materials. Res Mech 1988;24:99.
- [10] Meloun M, Militký J, Forina M. Chemometrics for analytic chemistry, vol. I: statistical data analysis. Chichester: Ellis Horwood; 1992.
- [11] Meloun M, Militký J, Forina M. Chemometrics for analytic chemistry, vol. II: regression and related Methods. Hempstead: Ellis Horwood; 1994.
- [12] Militký J. Proceedings of the 25th Textile Research Symposium at Mt. Fuji, August 1996.
- [13] Weddell JK. Continuous ceramic fibers. J Text Inst 1990;4:333.
- [14] Weibull W. J Appl Mech 1951;8:293.
- [15] Kies JA. NLR Report no. 5093, Naval Research Laboratory, Washington, DC; 1958.